ACCOUNTS
of chemical research

Theoretical Actinide Molecular Science

GEORG SCHRECKENBACH* AND GRIGORY A. SHAMOV
Department of Chemistry, University of Manitoba, Winnipeg, MB R3T 2N2, Canada

RECEIVED ON DECEMBER 17, 2008

CONSPECTUS

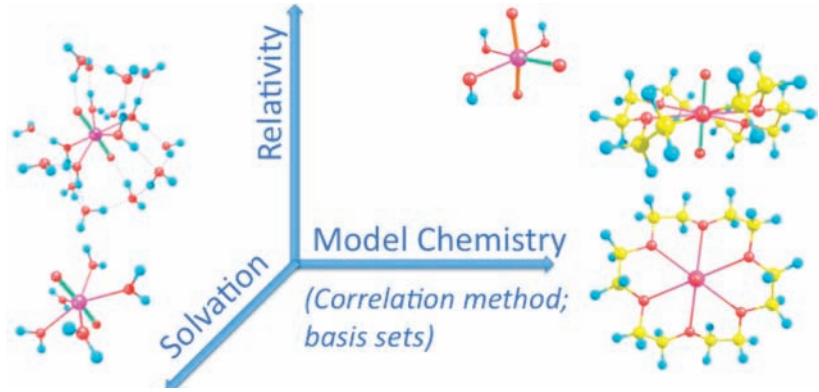

Interest in the chemistry of the early actinide elements (notably uranium through americium) usually results either from the nuclear waste problem or the unique chemistry of these elements that result from 5f contributions to bonding. Computational actinide chemistry provides one useful tool for studying these processes.

Theoretical actinide chemistry is challenging because three principal axes of approximation have to be optimized. These are the model chemistry (the choice of approximate electron−electron correlation method and basis sets), the approximate relativistic method, and a method for modeling solvent (condensed phase) effects. In this Account, we arrange these approximations in a three-dimensional diagram, implying that they are relatively independent of each other. A fourth level of approximation concerns the choice of suitable models for situations too complex to treat in their entirety. We discuss test cases for each of these approximations.

Gas-phase data for uranium fluorides and oxofluorides such as UF_6 and UO_2F_2 show that GGA functionals provide accurate geometries and frequencies while hybrid density functional theory (DFT) functionals are superior for energetics. MP2 is seen to be somewhat erratic for this set of compounds, and CCSD(T) gives the most accurate results. Three different relativistic methods, small-core effective core potentials (SC-ECP), ZORA, and all-electron scalar, provide comparable results. The older large-core ECP (LC-ECP) approach is consistently worse and should not be used. We confirmed these conclusions through studies of the actinyl aquo complexes $[AnO_2(OH_2)_5]^{n+}$, (An = U, Np, or Pu and $n = 1$ or 2) that are also used to test solvation models. As long as the first coordination sphere of the metal is included explicitly, continuum solvation models are reliable, and we found no clear advantage for the (costly) explicit treatment of the second coordination sphere. Spin−orbit effects must be included to reproduce the correct trend in An^{VI}/An^{V} reduction potentials.

We propose a multistep mechanism for the experimentally observed oxygen exchange of UO_2^{2+} cations in highly alkaline solutions present in tank wastes. This process involves an equilibrium between $[UO_2(OH)_4]^{2-}$ and $[UO_2(OH)_5]^{3-}$, followed by formation of the stable $[UO_3(OH)_3]^{3-}$ intermediate that forms from $[UO_2(OH)_5]^{3-}$ through intramolecular water elimination. The $[UO_3(OH)_3]^{3-}$ intermediate facilitates oxygen exchange through proton shuttling. We explain the experimentally observed stabilization of the pentavalent oxidation state of actinyl ions by macrocydic ligands (such as 18-crown-6) as an effect of solvation: the large macrocycle screens the positive charge of the ion from the polarizable solvent. Alkyl-substituted isoamethyrin complexes are bent despite being aromatic because of steric factors, rather than fit/misfit criteria regarding the actinyl ion.

By application of an efficient DFT code, actinide molecules with more than 100 atoms can now be studied routinely. "Real" chemical questions can be answered as long as we take great care to apply methods that are accurate with respect to the three axes of approximation described above. While the exclusive focus of this Account has been on the early actinide elements, these conclusions also apply elsewhere in the periodic table.

Published on the Web 08/31/2009 www.pubs.acs.org/acr
10.1021/ar800271r

Introduction: Actinide Chemistry—Why Bother?

One of the authors remembers vividly a colleague who, while teaching his class on transition metals, would tell his students: "And as far as the actinides are concerned, they aren't important, and you don't need to bother!" So *should* we bother?

If one asked any researcher why he or she is doing what he or she is doing, chances are that the answer is "because it's fun!" This is certainly true for our work in the area of theoretical actinide chemistry, and a purpose of this Account is to convey that "fun" to the reader. (It is not our intention to review the entire area of computational actinide chemistry.[1])

"Fun", however, is a category not normally employed in the scientific literature or in grant applications. The proper alternative term is "fundamental interest". *Fundamental interest* arises for a number of reasons, first and foremost among them the unique chemistry of the actinides.[2] Indeed, it is only here that f-orbitals play an appreciable role in bonding. This leads to unique bonding arrangements; uranocene provides a classic example.[3] Typical oxidation states for actinides range from 3 to 6 for uranium and 3 to 7 for neptunium and plutonium.[4] Coordination numbers as high as 12 are possible. In solution, complex equilibiria often exist, such as between mono- and polynuclear species, complicating experimental characterization.[5] Regarding challenges, we should not forget the radioactivity of the actinides that results in safety and security concerns, particularly for the transuranic elements.[6]

Computational actinide chemistry has its own challenges, arising from the combined effects of relativity and electron correlation, along with the size of typical systems, the large number of electrons, and the close energetic proximity of several electronic states. The actinides are still a frontier for applied quantum chemistry.

There is also *practical interest*, chiefly revolving around nuclear fuel processing, waste disposal, and long-term storage, as well as environmental cleanup of contaminated sites. Indeed, the nuclear waste problem, involving as it does time scales of the order of 100 000 years, is unsolved.[7] Contamination has resulted from more than six decades of nuclear weapons production and peaceful use of radioactivity. This is exemplified by the Hanford Site in Washington State, USA.[8] Radioactive contamination and cleanup can be considered one of the leading environmental challenges facing mankind.

It would be preposterous, of course, to pretend that a few calculations, however carefully done, might be key to solving the problem. Still, theory, particularly if approached in close interaction with experiment, has a unique chance of providing data, insight into, and understanding of the chemistry of the early actinide elements.

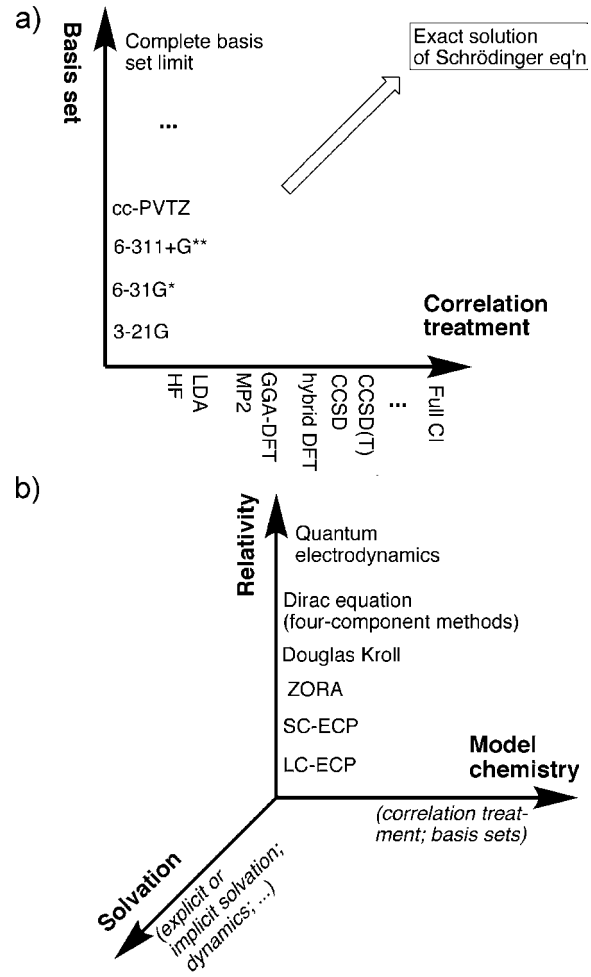

FIGURE 1. Schematic representation of (a) model chemistries according to Pople[11,12] and (b) three level of approximation required in computational actinide chemistry.

We shall, in the following, discuss a number of examples. We shall illustrate (i) the approximations that are needed and their evaluation and (ii) some applications. Finally, we shall summarize our conclusions.

Approximations

General. It is impossible in all but the simplest systems to solve the Schrödinger equation (or, in the case of relativistic quantum mechanics that has to be applied in actinide chemistry,[9] the Dirac equation[10]) exactly, and various approximations have to be chosen. These choices are at the heart of applied quantum chemistry.[11] We can only draw meaningful conclusions if we are sure that our approximate methods are applicable!

Textbooks often show a graph, attributed to John Pople,[12] that defines the "model chemistry", Figure 1a.[11] The graph has the approximate quantum-chemical method on one axis and

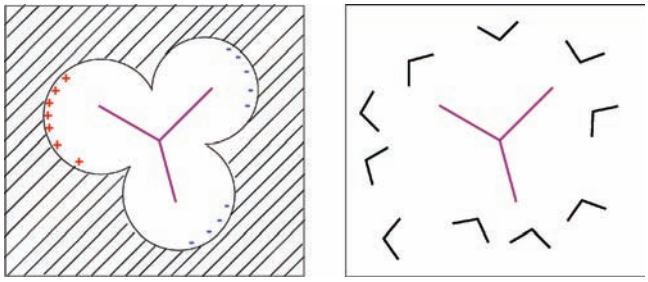

FIGURE 2. Schematic representation of continuum (left) and explicit (right) solvation models.

the basis set on the other. We propose to add two new axes, one for "relativity", that is, the approximate relativistic method, and another for "solvation", that is, the model used to account for the bulk solvent or, more generally, for condensed-phase effects. This is shown schematically in Figure 1b.[13] (We have combined the two axes of Figure 1a into one to fit the model into 3D space.) It is a reasonable assumption to consider the three levels of approximations to be relatively independent of each other, which allows us to test and optimize them separately. A further dimension might be the choice of a suitable model system for experimental systems that are too complex to be treated straightforwardly *in silico*.

Regarding the *model chemistry axis*, the only practical method in most cases is density functional theory (DFT),[14] given the size of experimentally relevant actinide systems. Still, there is considerable choice with respect to the flavor of approximate DFT, the exchange−correlation (XC) functional. Regarding basis sets, we can rely on the experience from other parts of the periodic table.[11]

A hierarchy of decreasing accuracy, supposedly combined with increasing efficiency, can be constructed for the *relativity axis*. Near the top is the full Dirac equation,[10] followed by two-component methods (e.g., the zeroth-order regular approximation for relativistic effects, ZORA[15]), and finally effective core potential (ECP) methods.[16,17] Spin−orbit effects can be projected out of the four- and two-component methods and neglected, leading to simpler scalar relativistic approximations.

It is less clear how to arrange the different methods on the *solvation axis*. The principal choices are explicit and continuum (implicit) solvation models, Figure 2. Continuum models replace the solvent by a polarizable continuum.[18] Various choices exist regarding size and shape of the solvent-excluded cavity and the parametrization of the solvent−solute interaction.[18] Explicit solvation models (microsolvation) include a finite number of solvent molecules. They are appealing since they avoid the ambiguities of the continuum methods, and they are probably unavoidable if direct solute−solvent bonds are important. Still, they have their own set of problems, resulting from the finite cluster sizes (How many solvent molecules? Surface effects?) and the difficulty in adequately sampling the large conformational space. Periodic or dynamic calculations might be required to overcome these two problems.[19] It is also possible to combine microsolvation and continuum methods.[20,21]

Test Case 1: Uranium Oxofluoride Gas-Phase Energetics. Accurate experimental gas-phase data is ideal for testing quantum-chemical methods since it allows one to focus on the *relativity* and *model chemistry* axes of Figure 1b. The general lack of such gas-phase experiments is a challenge for theoretical actinide molecular science. However, some data exists, and we have performed a study of the uranium(VI), uranium(V), and uranium(IV) oxides, fluorides, and oxofluorides.[22]

UF_6 is perhaps the most studied actinide molecule overall.[23] Table 1 shows its calculated[22,24] and experimental bond lengths and the first and second bond dissociation energies (BDE). The table also contains two other BDEs (UOF_4, UO_2F_2), chosen as representative examples, as well as statistical data for a total of 11 reactions. Vibrational frequencies have been studied also: for a given actinide, any trends in frequencies tend to follow trends in bond lengths quite closely. For instance, a method that overestimates bond lengths underestimates the corresponding stretching frequency.

We compare four different relativistic methods, as implemented in three different codes: all-electron scalar where the full Dirac equation is applied but with spin−orbit neglected (AE; Priroda[25]), ZORA[15] (ADF[26]), and large- and small-core ECP methods (LC-ECP,[16] SC-ECP;[17] Gausssian[27]). Two classes of approximate DFT are applied, generalized gradient approximations (GGA) and hybrid functionals. We have tested several functionals in each class but find the variations between these to be relatively minor. Hence, we only report one example each. We have also included standard correlated *ab initio* methods, MP2 and CCSD(T).

The data in Table 1 allows for a number of conclusions. First, comparing the older LC-ECP approach (14 valence electrons on uranium) with the SC-ECP method (32 valence electrons), we find that the latter is more accurate than the former. We demonstrate this here for UF_6, but it is a very general result (though it has been disputed,[28] in our view based on fortuitous error cancellation.) This is counterintuitive since the extra 18 electrons clearly occupy core shells. The likely reason for the differences between SC-ECPs and LC-ECPs is the following: When substituting the core by an effective potential, we create *by construction* pseudo-orbitals for the valence where the core wiggles (the orthogonality-imposed oscilla-

TABLE 1. Comparison between Selected Calculated and Experimental Parameters of UF_6, UF_5, UOF_4, and UO_2F_2 and MAE for 11 Reactions of Uranium Fluorides, Oxides, and Oxofluorides

		reaction enthalpies (kcal/mol)				
	bond lengths (Å), UF_6	$UF_6 \rightarrow UF_5 + F$	$UF_5 \rightarrow UF_4 + F$	$UOF_4 \rightarrow UF_4 + O$	$UO_2F_2 \rightarrow UO_2 + 2F$	MAE[a]
PBE, SC-ECP	2.024	107.1	127.4	134.9		38.6
PBE0, SC-ECP	1.997	80.6	105.1	97.8	254.6	17.2
PBE0, LC-ECP	2.006	30.1				
PBE, AE	2.015	100.5	120.8	132.6	266.2	24.6
PBE0, AE	1.990	73.6	97.8	95.3	241.9	6.9
MP2, AE[b]	2.005	84.0	97.8	120.9	249.9	13.2
CCSD(T), AE[c]		69.1	92.2	95.5	237.8	6.9
PBE, ZORA	2.025	101.5	126.6	137.7		23.9
experiment	1.996, 1.999	71.0	98.0	91.3	248.6	

[a] MAE = mean absolute error over 11 reactions with available experimental data.[22] Other choices of experimental data give slightly different errors; see Table S1, Supporting Information. [b] RI-MP2; all orbitals were correlated except for the first 30 orbitals on U and the 1s orbitals on F and O that are kept in core. [c] MP2 geometry, single-point calculations.

TABLE 2. Calculated (SC-ECP−B3LYP, LC-ECP−B3LYP; AE−PBE; Gas Phase) and Experimental Bond Lengths (Å) of $[AnO_2(H_2O)_5]^{n+}$ [a]

	$[UO_2(H_2O)_5]^{2+}$				$[NpO_2(H_2O)_5]^{2+}$				$[PuO_2(H_2O)_5]^{2+}$			
	SC-ECP−B3LYP	LC-ECP−B3LYP	AE−PBE	expt[b]	SC-ECP−B3LYP	LC-ECP−B3LYP	AE−PBE	expt[b]	SC-ECP−B3LYP	LC-ECP−B3LYP	AE−PBE	expt[b]
$R_{An=O}$	1.751	1.756	1.776	1.76; *1.78*	1.730	1.752	1.758	1.75; 1.76	1.720	1.742	1.749	1.74
R_{An-O_eq}[c]	2.486	2.516	2.472	2.41	2.470	2.50	2.457	2.42; *2.42*	2.466	2.485	2.453	2.41
	$[UO_2(H_2O)_5]^{1+}$				$[NpO_2(H_2O)_5]^{1+}$				$[PuO_2(H_2O)_5]^{1+}$			
	SC-ECP−B3LYP	LC-ECP−B3LYP	AE−PBE	expt[b]	SC-ECP−B3LYP	LC-ECP−B3LYP	AE−PBE	expt[b]	SC-ECP−B3LYP	LC-ECP−B3LYP	AE−PBE	expt[b]
$R_{An=O}$	1.806	1.810	1.824		1.791	1.81	1.807; 1.810	1.83; *1.84*	1.776	1.808	1.796; 1.797	1.81
R_{An-O_eq}[c]	2.585	2.616	2.568		2.588	2.61	2.567	2.50; 2.52; *2.49*	2.577	2.61	2.567	2.47

[a] An = U, Np, Pu; n = 1, 2. (See Table S3, Supporting Information, for frequencies.). [b] As cited in refs 20 and 30, new neptunium data[31] added in italics. [c] Average.

tions and nodes of valence orbitals) are smoothed out and removed. By unfreezing one entire shell of core orbitals, we add back the outermost core wiggle to the valence orbitals. This core wiggle may reach into regions of space that are relevant for bonding. Thus, the effect of the extra 18 electrons in the SC-ECPs would be an indirect one in that they force a more accurate description of the valence oribtals. It has been argued that the neglect (or approximate treatment) of core polarization and correlation might be relevant, too.

Comparing now the different relativistic approximations SC-ECP, ZORA, and AE, we find them to give similar results, provided the same DFT method (e.g., PBE in Table 1) is used and the basis sets are reasonably converged.[29] This is reassuring. The three methods take very different approaches to the "relativity axis" of Figure 1b. Agreement among them, then, would mean that they can be used interchangeably and that the description of relativity is essentially correct, at least for the kind of valence properties considered here and under the caveat that spin−orbit effects are neglected (see also below.)

Let us now turn to the "model chemistry" axis of Figure 1. We have modeled dissociation of covalent U−F and U═O bonds in uranium oxofluorides; selected results are shown in Table 1.[22] Hybrid DFT (PBE0) is superior to pure GGAs (PBE) for the energetics; at the same time, hybrids show bond lengths that are too short and frequencies that are too high (overbinding; GGAs improve on that); this is again a very general result. Over the whole set of uranium oxofluoride compounds, MP2 shows somewhat "erratic" results; that is, for example, it does overbind U−F bonds for the highly fluorinated species UF_6 but not for UO_2F_2. The overall agreement for MP2 energies is better than for GGAs but slightly worse than for hybrid functionals. For wave function based methods, only CCSD(T) gave consistently the best reaction enthalpies.

Test Case 2: Actinyl Aquo Complexes. The actinyl aquo complexes $[AnO_2(H_2O)_5]^{n+}$ (n = 1, 2) are prototypical environmental actinide species, since environmental chemistry implies aqueous environments. They provide a fertile testing ground for all three levels of approximation, model chemistry, relativity, and solvation, Figure 1b. The challenge lies in separating the different effects.

In Table 2 and Table S3 of the Supporting Information, we compare computed bond lengths and actinyl frequencies to experiment.[20,30,31] An example of an optimized structure is shown in Figure 3. Regarding methods, we can draw essentially the same conclusions as before: LC-ECP is consistently inferior to the other relativistic methods. B3LYP tends to overbind. (There is some measure of error compensation visible in the LC-ECP−B3LYP data.) PBE gives the best bond

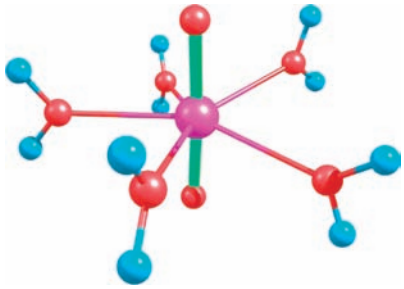

FIGURE 3. Optimized gas-phase structure (AE−PBE) of $[UO_2(H_2O)_5]^{2+}$.[20]

lengths, particularly for equatorial bonds, though they are still overestimated by these gas-phase calculations.

In going from left to right along the actinide series (U to Np to Pu), the actinide contraction is clearly evident from the data: The actinyl bond becomes both shorter and weaker along the series, due to the decreasing size of the f-orbitals and thus decreasing covalent character of the bonds.[20,30,31]

The uranyl aquo complexes provide us with an opportunity to test explicit and implicit solvation models for structures, frequencies, and energetics (Tables S4 and S5, Supporting Information). Explicit solvation, Figure 2b, has been modeled by adding five, seven, ten, and twelve water molecules to the second coordination sphere (Figure 4). These structures can be embedded into continuum solvation. Several conclusions emerge:

- Solvation strongly influences the bond lengths, particularly the equatorial bonds that are overestimated by gas-phase calculations. The effect is evident for both explicit and implicit solvation models; the effect on the frequencies is similar.
- The second coordination sphere has only a minor effect on the energetics.

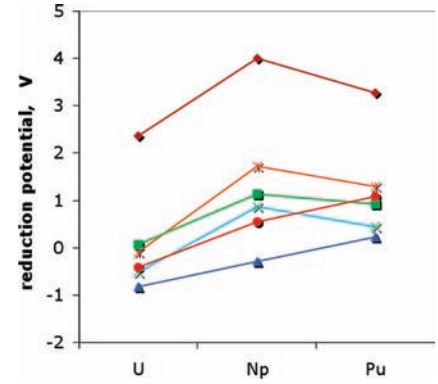

FIGURE 5. Calculated and experimental $[AnO_2(H_2O)_5]^{2+}/[AnO_2(H_2O)_5]^{1+}$ reduction potentials.[20,30] Calculated values without and with the inclusion of (empirical) spin−orbit and multiplet corrections are shown. Green squares, experiment; dark red diamonds, LC-ECP−B3LYP with corrections; red circles, SC-ECP−B3LYP without corrections; blue triangles, AE−PBE without corrections; orange stars, SC-ECP−B3LYP with corrections; light blue crosses, AE−PBE with corrections.

- Cluster models (explicit solvation) are unable to capture long-range electrostatic effects on the energetics.
- Overall, no clear advantage for combined methods (second coordination sphere plus continuum solvation) can be seen. We note, however, that others disagree.[21]

In Figure 5, we show the calculated reduction potentials for the An^{VI}/An^{V} couples. In our earlier LC-ECP studies,[30] we already recognized the importance of spin−orbit and multiplet corrections that are not accounted for by approximate scalar DFT. These are required to reproduce the correct trend in relative reduction potentials, for example, dark vs light blue lines, Figure 5. (We note in passing that the same trend in relative reduction potentials is evident for other ligand environments also;[32] it is thus primarily a function of the actinyl ion.) However, we were unable to remove the

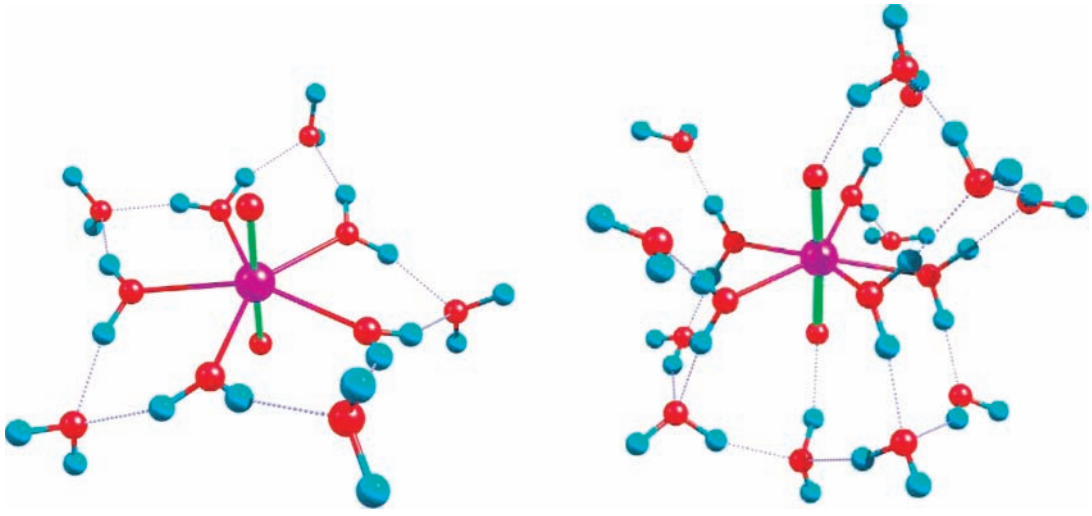

FIGURE 4. Two examples of explicitly solvated complexes: optimized structures of $[UO_2(H_2O)_5]^{2+}\cdot 5H_2O$ and $[UO_2(H_2O)_5]^{2+}\cdot 12H_2O$ (AE−PBE gas phase).[20]

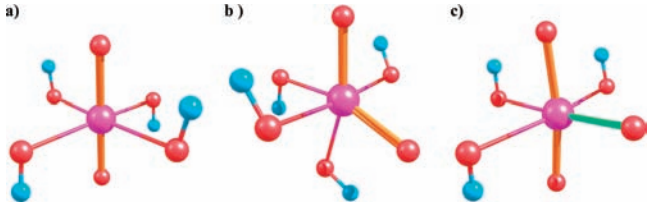

FIGURE 6. Optimized structures of (a) trans and (b) cis isomer of $[UO_2(OH)_4]^{2-}$, and (c) the new oxygen exchange intermediate $[UO_3(OH)_3]^{3-}$.

large systematic error of some 3 eV (dark red line) that could have been due to any of the different levels of approximation in Figure 1b. This has been solved recently; the relativistic approximation was the main problem.[20] Both AE and SC-ECPs give dramatically better results. Interestingly, in this example, there is no clear advantage for either hybrid or GGA DFT.

Uranyl Hydroxide: Ligand Exchange, *cis*-Uranyl Structures

Highly alkaline conditions are prevalent for tank wastes, and uranyl hydroxide, $[UO_2(OH)_4]^{2-}$, is a prototypical species, Figure 6. This molecule has been synthesized and characterized by Clark and co-workers[33] who used a bulky counterion to prevent formation of insoluble higher aggregates. Several intriguing questions arise. The equatorial coordination number has been controversial, with four or five being the possibilities. Most interestingly, a rapid ligand exchange between axial and equatorial oxygens has been observed ($\Delta H^{\ddagger} = 9.8$ kcal/mol). This is highly unusual, given the known stability of the uranyl unit.[4] The process has escaped a plausible mechanistic explanation until very recently.

The first mechanistic proposal was provided in the original paper,[33] a concerted movement of two hydrogens (Scheme 1a). We have tested this proposal computationally and found a barrier of 58.6 kcal/mol.[34] Moreover, the transition state is a second-order saddle point. This led us to test a revised mechanism where only one hydrogen atom is moved in pseudorotation, Scheme 1b. This mechanism necessitates a stable intermediate with a bent uranyl unit, termed "*cis*-uranyl", Figure 6b. We note in passing that, based on our proposal, several experimental groups attempted to synthesize stable *cis*-uranyl structures. This search has succeeded only recently.[35]

The calculated gas-phase activation energy for the pseudorotation mechanism is 37.5 kcal/mol at the LC-ECP–B3LYP level of theory that was still used at the time. Explicit inclusion of a water molecule into the proton shuttle

SCHEME 1. Oxygen Exchange in Uranyl Hydroxide, Previous Mechanistic Proposals[33,34]

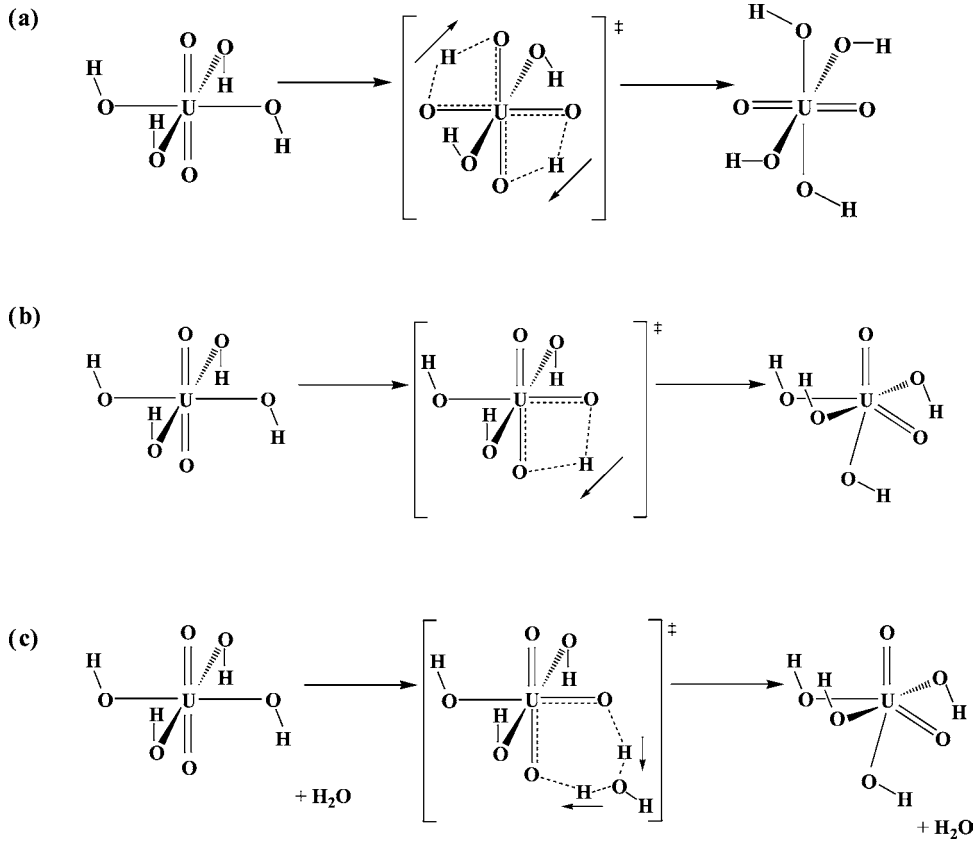

(Scheme 1c) reduces the activation energy to 31.4 kcal/mol. Adding continuum solvation reduces it by a further 5 kcal/mol or so. Still, the best calculated activation energy of 26.8 kcal/mol does not provide a satisfactory explanation for the experimentally observed process. (Using modern relativistic methods or different solvation models lowers the barrier further but does not fundamentally change the qualitative picture.[36])

This was the state of our investigations in about 2000, when we essentially shelved the subject as unsolved. Fairly recently, though, we realized that the problem of the pseudorotation mechanism lies in the fact that it contains a *cis*-intermediate and that it requires the system to give up the tremendous energetic advantages of the linear uranyl unit. Is it possible, then, to modify the process to retain a linear uranyl throughout? An $[UO_3(OH)_3]^{3-}$ intermediate as facilitator of the exchange could satisfy the condition. The full mechanism is provided in Scheme 2. The first step of the new mechanism,

$$[UO_2(OH)_4]^{2-} + OH^- \leftrightarrow [UO_2(OH)_5]^{3-} \quad (1)$$

concerns the experimentally observed equatorial coordination equilibrium in solution. The next step involves elimination of a water molecule to form the key $[UO_3(OH)_3]^{3-}$ intermediate:

$$[UO_2(OH)_5]^{3-} \rightarrow [UO_3(OH)_3]^{3-} + H_2O \quad (2)$$

This process has a low activation barrier and goes steeply downhill. It thus drives the equatorial equilibrium 1 to the right-hand side, particularly under the experimental conditions of alkaline solutions and high ionic strength of NaOH. The $[UO_3(OH)_3]^{3-}$ intermediate facilitates the oxygen ligand exchange through proton shuttling, either without or with an explicit water molecule (4a, 4b in Scheme 2):

SCHEME 2. Oxygen Exchange in Uranyl Hydroxide, Proposed Three-Step Mechanism[36]

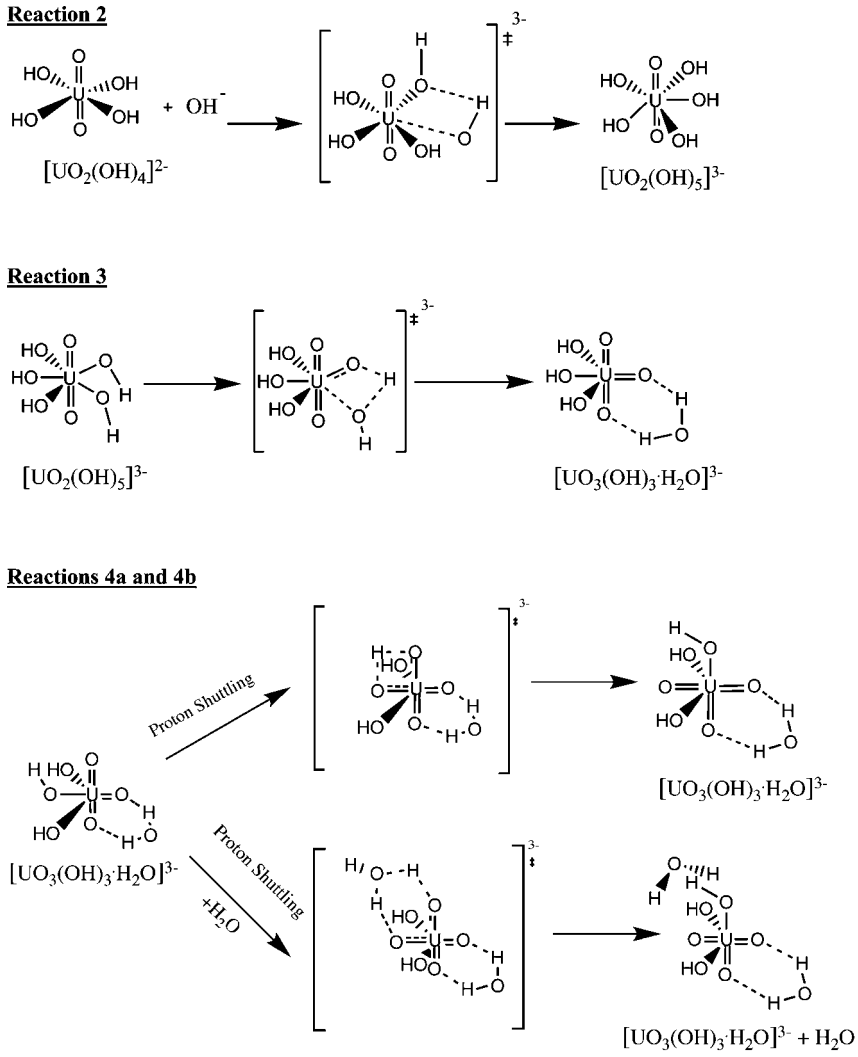

$$[O{=}U{=}O^*(O)(OH)_3]^{3-} \leftrightarrow [UO_2(O)(O^*H)(OH)_2]^{3-} \quad (3)$$

The overall calculated activation energy, 12.5 kcal/mol for the initial step (eq 1), compares favorably to the experimental value of 9.8 kcal/mol, particularly because it appears to be stable against methodological variations. The proposed mechanism, reactions 2−4, Scheme 2, is therefore a plausible explanation of the experimental observations, solving a 10-year-old riddle.

Crown Ether Complexes: Why Do Macrocycles Stabilize the Pentavalent Oxidation State?

Clark et al. synthesized and characterized the first *trans*-uranic crown ether inclusion complex $[NpO_2(18\text{-crown-6})]^{1+}$.[37] We have studied this system,[38] along with its $An^{V/VI}$ counterparts (An = U, Np, Pu) and related uranyl complexes synthesized earlier. Figure 7 shows an example for an optimized structure. We note again the effect of the actinide contraction, that is, actinyl bond lengths that become shorter and weaker along the actinide series (see Table S6, Supporting Information).

The most intriguing question in Clark's paper concerns the observation that macrocycles such as 18-crown-6 stabilize the An^{V} oxidation state over An^{VI}, thus perhaps allowing for selective extraction of specific metals in specific oxidations states. It has been speculated[39] that this stabilization comes about because "reduction from oxidation state VI to V gives an expanded metal ion radius that provides a better fit to the [ligand] cavity". To probe the origins of the stabilization effects, we have chosen two reactions, the complex formation reaction 4 and the ligand exchange reaction 5.[38]

$$AnO_2^{n+} + 18\text{-crown-6} \rightarrow [AnO_2(18\text{-crown-6})]^{n+} \quad (4)$$

$$[AnO_2(H_2O)_5]^{n+} + 18\text{-crown-6} \rightarrow [AnO_2(18\text{-crown-6})]^{n+} + 5H_2O \quad (5)$$

(An = U, Np, or Pu and n = 1 or 2). Reaction 5 might be closer to the experimental situation. It accounts in an approximate manner for the competition between outer-sphere and inner-sphere complexes. Calculated free energies are provided in Table 3.

If the interaction between actinyl ion and macrocycle (the "fit/misfit" criteria) was the driving force for the stabilization of An^{V}, then this would be evident from the gas-phase data. This is not the case. Instead, ΔG for An^{V} is very roughly half that of the respective An^{VI} counterpart for both reactions. This can be understood from the charges of the cations, 1+ vs 2+, because the equatorial bonds are primarily ionic in character.[38]

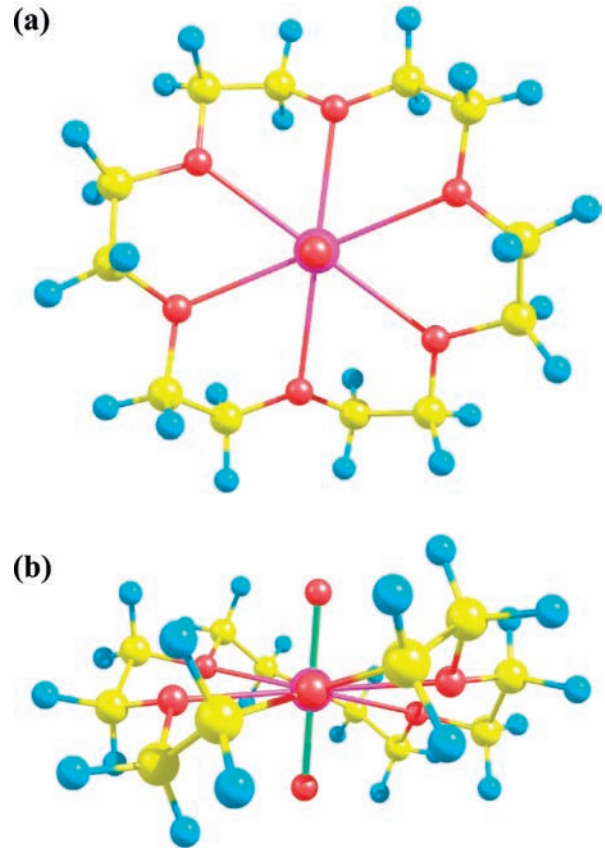

FIGURE 7. Optimized structure of $[UO_2(18\text{-crown-6})]^{2+}$: (a) top and (b) side views.[38]

TABLE 3. Reaction Energies for Reactions 4 and 5 in kcal/mol[38]

		reaction 5[a]				
			$\Delta\Delta G^{solv}$		ΔG(aq)	
	reaction 4, ΔG(gas)	ΔG(gas)	CPCM	COSMO-PCM	CPCM	COSMO-PCM
$[UO_2]^{2+}$	−273.8	−62.2	58.4	37.2	12.0	−9.3
$[UO_2]^{1+}$	−121.7	−33.7	28.5	12.8	3.5	−12.3
$[NpO_2]^{2+}$	−266.4	−59.5	58.9	37.3	11.5	−10.1
$[NpO_2]^{1+}$	−121.6	−38.0	26.9	12.3	3.6	−11.1
$[PuO_2]^{2+}$	−267.8	−64.4	58.5	28.2	24.2	−6.2
$[PuO_2]^{1+}$	−120.5	−38.3	27.6	11.1	5.4	−11.1

[a] The $5H_2O$ term on the right-hand side of reaction 5 has been treated as a cluster, $(H_2O)_5$.

For the free energies in solution, however, $\Delta\Delta G^{solv}$ is large and positive in all cases. Solvation strongly favors the left-hand side of reaction 5. This can be readily understood: To first order, solvation stabilizes a charged solute by polarization of the polar solvent. The effect is proportional to the charge squared and inversely proportional to the distance between charge and polarizable medium. The charge is balanced; however, the distance to the solvent is quite different for the left- and right-hand sides of reaction 5. In other words, the large macrocycle screens the charge, leading to a positive $\Delta\Delta G^{solv}$. The effect is much stronger for the 2+ charge of An^{VI} complexes than for the 1+ charge of An^{V} systems. This,

SCHEME 3

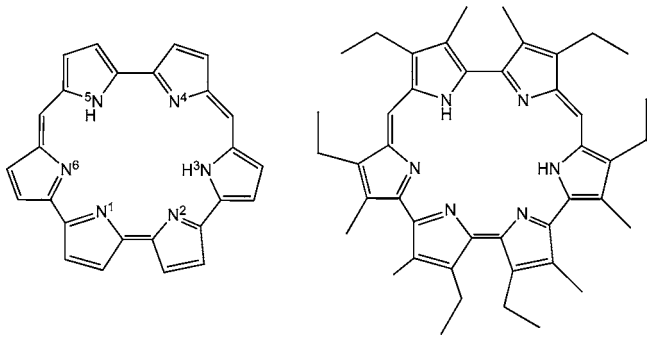

in turn, leads to the *relative* stabilization of the pentavalent oxidation state.[40]

Isoamethryin Complexes: Bent or Planar?

N-donor macrocyclic ligands, expanded porphyrins, constitute another class of macrocycles that possess a great variety in size and electronic properties. They can in principle be tailored to different metal ions.[41] Actinide complexes with expanded porphyrins have been studied both experimentally[42,43] and theoretically.[32,44−46]

As an example, we shall discuss our work on the unsubstituted and substituted isoamethyrin complexes, Scheme 3 and Figure 8.[45] The macrocyclic ligand is aromatic, so one would expect a planar structure. However, the experimentally obtained complexes of uranyl(VI) and neptunyl(V) dodeca-alkyl substituted isoamethryrin complexes show a nonplanar conformation.[47] The authors speculate[47] that the bending is "a result of a need to accommodate a metal center that is slightly too small." We have addressed this question by also studying uranyl complexes of the unsubstituted system, as well as the free ligand. Having compared the dodeca-alkyl substituted ligand and its uranyl complexes with their unsubstituted counterparts, we found that the ligand bending is due to steric repulsion of the ligand's peripheral alkyl groups and that it shows up already in the free ligand but is absent from either the free or complexed unsubstitued ring. The ligand bending indeed allows for a better "fit" to the uranyls (both uranyl(V) and uranyl(VI)) because it provides shorter, more optimal uranium-to-nitrogen distances than those possible in the planar isoamethyrin ligand.

Conclusions

With application of an efficient DFT code, actinide molecules with well over 100 atoms can now be studied routinely. This makes it possible to gain unique insight by connecting the calculated properties to details of the electronic structure. Thus, "real" chemical questions can be answered, provided great care is taken to apply methods that are accurate with respect to every single axis of Figure 1b. While the exclusive focus of this Account has been on the early actinide elements, these conclusions apply of course elsewhere in the periodic table also.

Methods. Regarding methods, we draw the following specific conclusions:

- Three different scalar *relativistic methods*, AE, ZORA, and SC-ECP, give very close results, provided all other settings are similar.[20,22] Therefore, these relativistic method can be considered as accurate, at least as far as valence properties are concerned. The older LC-ECP method is consistently worse than other relativistic methods and should probably not be used anymore.[20,30,38]
- *Spin−orbit effects* are relevant for properties such as reduction or oxidation energies or potentials and NMR chemical shifts.[20,22,24,30]
- *Hybrid* DFT gives much better energetics than *GGA* functionals for covalent bond-breaking, for example, in the case of uranyl oxofluorides. For weaker coordinative bonds like those in aqua-complexes, both approaches give comparable energies. At the same time, though, hybrids tend to overbind, as is evident from bond lengths and frequencies. GGA functionals perform, in general, better for these

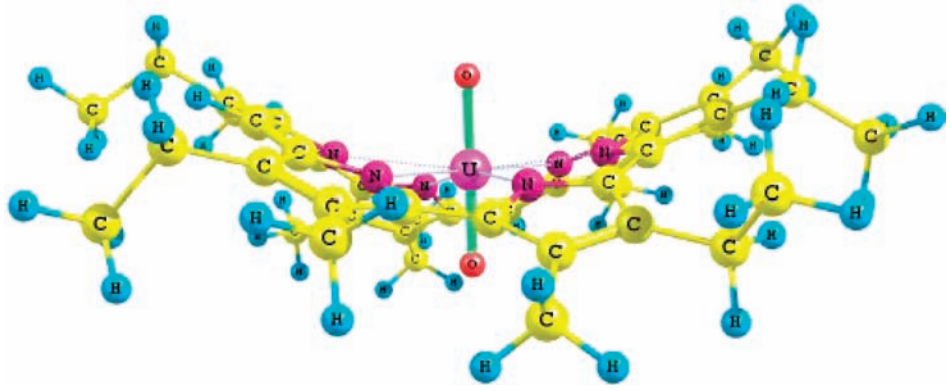

FIGURE 8. Optimized structure of the dodeca-alkyl-substituted isoamethyrin uranyl complex.[45]

properties.[20,22] This kind of situation is, of course, not entirely satisfactory, because one would prefer a universally applicable method. Modern incarnations of both hybrids and GGAs, and new developments such as meta-GGAs should probably be included into benchmark studies.[11]

- *Solvation effects* are very important.[20,38] Continuum solvation models appear to work reasonably well, provided the first coordination sphere is treated explicitly. These models do depend (too) strongly on the choice of atomic radii, though. We have not found any clear advantage for an explicit second solvation shell (others have concluded differently[21]), particularly given the additional problems that arise from this approach.[20]
- In general, great care has to be taken regarding *all levels of approximations* including the choice of model; otherwise, meaningful conclusions might be impossible.

Applications. Some specific conclusions on different systems are as follows:

- The uranyl(VI) hydroxide system has been studied extensively. We have proposed stable *cis*-uranyl isomers[34] that have only recently been realized experimentally.[35] The experimentally observed oxo ligand exchange has been explained by a three-step mechanism with $[UO_3(OH)_3]^{3-}$ as a key intermediate, Scheme 2.[36]
- We have shown that the experimentally observed stabilization of the pentavalent metal oxidation state by crown ethers[37] is entirely an effect of solvation and not of fit or cavity size.[38]
- Theory is capable of probing questions such as the reason for conformational preferences. The observed[45] nonplanar conformation of inclusion complexes of substituted isoamethyrin, Figure 8, is purely a steric effect of the peripheral alkyl ligands.[45]

Overall, we hope that we have conveyed a sense that relativistic DFT is a reliable tool for the study of actinide molecules!

Financial support from NSERC and the University of Manitoba is gratefully acknowledged.

Supporting Information Available. Reactions used in the statistical analysis in Table 1, raw data for this statistical analysis (Tables S1, S2), extended version of Table 2 (Table S3), bond lengths, frequencies (Table S4), and energetics (Table S5) for explicitly solvated aquo complexes, and bond lengths, bond orders, and frequencies for crown ether complexes (Table S6). This material is available free of charge via the Internet at http://pubs.acs.org.

BIOGRAPHICAL INFORMATION

Georg Schreckenbach was born in 1965 in Potsdam, (East) Germany. He studied physics in Dresden, before going to the University of Calgary, Canada, where he obtained his Ph.D. in 1996 under the supervision of Tom Ziegler. From 1997 to 2000, he was Seaborg Institute Postdoctoral Fellow at Los Alamos National Laboratory (USA). After a period at Daresbury Laboratory, U.K., he joined Concordia University (Montreal, Canada) as an Assistant Professor in 2001. In 2003, he came to the University of Manitoba where he is currently Associate Professor of Chemistry. Dr. Schreckenbach's research involves developing and applying density functional methods to diverse problems such as NMR, actinide chemistry, homogeneous catalysis, mercury complexes, hydroxyproline derivatives, or dye-sensitized solar cells.

Grigory A. Shamov was born in 1975 in Kazan, Russia. He studied chemistry at the Kazan State University, where in 1997 he got his Diplom in Chemistry and in 2000 obtained his Ph.D. degree under the supervision of Andrey Vedernikov, in the area of DFT modeling of alkane C−H bond activation by platinum metal complexes. Starting in 2001 he worked as a research associate at Kazan Science Centre of the Russian Academy of Science. In 2004−2006 he was a postdoctoral fellow at the University of Manitoba, under the supervision of Prof. Schreckenbach. Following a stay as research associate at Technical University of München, Germany, with Prof. Notker Rösch in 2006−2007, he is now a research associate at the University of Manitoba. Dr. Shamov's research interests are in theoretical modeling of actinide chemistry, mechanisms of organic and organometallic reactions, and homogeneous catalysis.

FOOTNOTES

*To whom correspondence should be addressed. E-mail: schrecke@cc.umanitoba.ca.

REFERENCES

1 Kaltsoyannis, N.; Hay, P. J.; Li, J.; Blaudeau, J. P.; Bursten, B. E. Theoretical Studies of the Electronic Structure of Compounds of the Actinides. In *The Chemistry of the Actinide and Transactinide Elements*, 3rd ed.; Morss, L. R., Edelstein, N. M., Fuger, J., Katz, J. J., Eds.; Springer: Dordrecht, The Netherlands, 2006; Vol. 3, pp 1893−2012.

2 *The Chemistry of the Actinide and Transactinide Elements*, 3rd ed.; Morss, L. R., Edelstein, N. M., Fuger, J., Katz, J. J. ,Eds.; Springer: Dordrecht, The Netherlands, 2006.

3 Streitwieser, A.; Müller-Westhof, U. Bis(cyclooctatetraenyl)uranium (uranocene). A new class of sandwich complexes that utilize atomic f orbitals. *J. Am. Chem. Soc.* **1968**, *90*, 7364.

4 Kaltsoyannis, N.; Scott, P. *The F Elements*; Oxford University Press: New York, 1999.

5 Choppin, G. R.; Jensen, M. P. Actinides in Solution: Complexation and Kinetics. In *The Chemistry of the Actinide and Transactinide Elements*, 3rd ed.; Morss, L. R., Edelstein, N. M., Fuger, J., Katz, J. J., Eds.; Springer: Dordrecht, The Netherlands, 2006; Vol. 4, pp 2524−2621.

6 In principle, a few kilograms of plutonium are sufficient to build a nuclear weapon.

7 Haschke, J. M.; Stakebake, J. L. Handling, Storage, and Disposition of Plutonium and Uranium. In *The Chemistry of the Actinide and Transactinide Elements*, 3rd ed.; Morss, L. R., Edelstein, N. M., Fuger, J., Katz, J. J., Eds.; Springer: Dordrecht, The Netherlands, 2006; Vol. 5, pp 3199−3272.

8 The Hanford site (http://www.hanford.gov/) had been used for plutonium production for some 40 years. It is the most radioactively contaminated site in the USA, containing 9 decommissioned reactors, over 200,000 m^3 of high-level mixed waste in underground tanks (some of which are believed to be leaking), etc. One can only speculate about the magnitude of the contamination in other countries with a history of nuclear weapons production.

9 Pyykkö, P. Relativistic Effects in Structural Chemistry. *Chem. Rev.* **1988**, *88*, 563–594.

10 Dirac, P. A. M. The Quantum Theory of the Electron. *Proc. R. Soc. London, Ser. A* **1928**, *117*, 610.

11 Cramer, C. J. *Essentials of Computational Chemistry: Theories and Models*, 2nd ed.; Wiley: New York, 2004.

12 Pople, J. A. Two-Dimensional Chart of Quantum Chemistry. *J. Chem. Phys.* **1965**, *43*, S229–S230.

13 The idea of "relativity as the third dimension" has been put forward by others also, for example, http://www.chem.vu.nl/~visscher/PDFs/2007_ESQC.pdf.

14 Koch, W.; Holthausen, M. C. *A Chemist's Guide to Density Functional Theory*; Wiley Verlag Chemie: New York, 2000.

15 van Lenthe, E.; Baerends, E. J.; Snijders, J. G. Relativistic Regular Two-Component Hamiltonians. *J. Chem. Phys.* **1993**, *99*, 4597–4610.

16 Hay, P. J.; Martin, R. L. Theoretical Studies of the Structure and Vibrational Frequencies of Actinide Compounds Using Relativistic Effective Core Potentials with Hartree-Fock and Density Functional Methods. UF_6, NpF_6 and PuF_6. *J. Chem. Phys.* **1998**, *109*, 3875–3881.

17 Küchle, W.; Dolg, M.; Stoll, H.; Preuss, H. Energy-Adjusted Pseudopotentials for Actinides: Parameter Sets and Test Calculations for Thorium and Thorium Monooxide. *J. Chem. Phys.* **1994**, *100*, 7535–7542.

18 Cramer, C. J.; Truhlar, D. G. Implicit Solvation Models: Equilibria, Structure, Spectra, and Dynamics. *Chem. Rev.* **1999**, *99*, 2161–2200.

19 Bühl, M.; Kabrede, H.; Diss, R.; Wipff, G. Effect of Hydration on Coordination Properties of Uranyl(VI) Complexes. A First-Principles Molecular Dynamics Study. *J. Am. Chem. Soc.* **2006**, *128*, 6357–6368.

20 Shamov, G. A.; Schreckenbach, G. Density Functional Studies of Actinyl Aquo Complexes Studied Using Small-Core Effective Core Potentials and a Scalar Four-Component Relativistic Method. *J. Phys. Chem. A* **2005**, *109*, 10961–10974. Correction: Shamov, G. A.; Schreckenbach, G. Density Functional Studies of Actinyl Aquo Complexes Studied Using Small-Core Effective Core Potentials and a Scalar Four-Component Relativistic Method. *J. Phys. Chem. A* **2006**, *110*, 12072.

21 Gutowski, K. E.; Dixon, D. A. Predicting the Energy of the Water Exchange Reaction and Free Energy of Solvation for the Uranyl Ion in Aqueous Solution. *J. Phys. Chem. A* **2006**, *110*, 8840–8856.

22 Shamov, G. A.; Schreckenbach, G.; Vo, T. A Comparative Relativistic DFT and Ab Initio Study on the Structure and Thermodynamics of the Oxofluorides of Uranium(IV), (V) and (VI). *Chem.—Eur. J.* **2007**, *13*, 4932–4947.

23 To perform calculations on UF_6 appears to almost be a "rite of passage" for entering the actinide field!

24 Schreckenbach, G.; Hay, P. J.; Martin, R. L. Density Functional Calculations on Actinide Compounds. Survey of Recent Progress and Application to $[UO_2X_4]^{2-}$ (X = F, Cl, OH) and AnF_6 (An = U, Np, Pu). *J. Comput. Chem.* **1999**, *20*, 70–90.

25 Laikov, D. N.; Ustynyuk, Y. A. PRIRODA-04: A Quantum-Chemical Program Suite. New Possibilities in the Study of Molecular Systems with the Application of Parallel Computing. *Russ. Chem. Bull.* **2005**, *54*, 820–826.

26 te Velde, G.; Bickelhaupt, F. M.; Baerends, E. J.; Fonseca Guerra, C.; van Gisbergen, S. J. A.; Snijders, J. G.; Ziegler, T. Chemistry with ADF. *J. Comput. Chem.* **2001**, *22*, 931–967.

27 Frisch, M. J.; Trucks, G. W.; Schlegel, H. B.; Scuseria, G. E.; Robb, M. A.; Cheeseman, J. R.; Montgomery, J. A., Jr.; Vreven, T.; Kudin, K. N.; Burant, J. C.; Millam, J. M.; Iyengar, S. S.; Tomasi, J.; Barone, V.; Mennucci, B.; Cossi, M.; Scalmani, G.; Rega, N.; Petersson, G. A.; Nakatsuji, H.; Hada, M.; Ehara, M.; Toyota, K.; Fukuda, R.; Hasegawa, J.; Ishida, M.; Nakajima, T.; Honda, Y.; Kitao, O.; Nakai, H.; Klene, M.; Li, X.; Knox, J. E.; Hratchian, H. P.; Cross, J. B.; Bakken, V.; Adamo, C.; Jaramillo, J.; Gomperts, R.; Stratmann, R. E.; Yazyev, O.; Austin, A. J.; Cammi, R.; Pomelli, C.; Ochterski, J. W.; Ayala, P. Y.; Morokuma, K.; Voth, G. A.; Salvador, P.; Dannenberg, J. J.; Zakrzewski, V. G.; Dapprich, S.; Daniels, A. D.; Strain, M. C.; Farkas, O.; Malick, D. K.; Rabuck, A. D.; Raghavachari, K.; Foresman, J. B.; Ortiz, J. V.; Cui, Q.; Baboul, A. G.; Clifford, S.; Cioslowski, J.; Stefanov, B. B.; Liu, G.; Liashenko, A.; Piskorz, P.; Komaromi, I.; Martin, R. L.; Fox, D. J.; Keith, T.; Al-Laham, M. A.; Peng, C. Y.; Nanayakkara, A.; Challacombe, M.; Gill, P. M. W.; Johnson, B.; Chen, W.; Wong, M. W.; Gonzalez, C.; Pople, J. A. *Gaussian 03*, revision C.02; Gaussian, Inc.: Wallingford, CT, 2004.

28 Iche-Tarrat, N.; Marsden, C. J. Examining the Performance of DFT Methods in Uranium Chemistry: Does Core Size Matter for a Pseudopotential? *J. Phys. Chem. A* **2008**, *112*, 7632–7642.

29 Basis set convergence has been established for the different codes in our original paper. Most critically, this has been an issue for the G03 calculations: the commonly used 6-31G** ligand basis is insufficient.

30 Hay, P. J.; Martin, R. L.; Schreckenbach, G. Theoretical Studies of the Properties and Solution Chemistry of AnO_2^{2+} and AnO_2^{+} Aquo Complexes for An = U, Np, Pu. *J. Phys. Chem. A* **2000**, *104*, 6259–6270.

31 Ikeda-Ohno, A.; Hennig, C.; Rossberg, A.; Funke, H.; Scheinost, A. C.; Bernhard, G.; Yaita, T. Electrochemical and Complexation Behavior of Neptunium in Aqueous Perchlorate and Nitrate Solutions. *Inorg. Chem.* **2008**, *47*, 8294–8305.

32 Berard, J. J.; Schreckenbach, G.; Arnold, P. L.; Patel, D.; Love, J. B. Computational DFT Study of Polypyrrolic Macrocycles: Analysis of Actinyl-Oxo to Transition Metal Bonding. *Inorg. Chem.* **2008**, *47*, 11583–11592.

33 Clark, D. L.; et al. Chemical Speciation of the Uranyl Ion Under Highly Alkaline Conditions. Synthesis, Structure and Oxo Ligand Exchange Dynamics. *Inorg. Chem.* **1999**, *38*, 1456–1466.

34 Schreckenbach, G.; Hay, P. J.; Martin, R. L. Theoretical Study of Stable Trans and Cis Isomers in $[UO_2(OH)_4]^{2-}$ Using Relativistic Density Functional Theory. *Inorg. Chem.* **1998**, *37*, 4442–4451.

35 Vaughn, A. E.; Barnes, C. L.; Duval, P. B. A cis-Dioxido Uranyl: Fluxional Carboxylate Activation from a Reversible Coordination Polymer. *Angew. Chem., Int. Ed.* **2007**, *46*, 6622–6625.

36 Shamov, G. A.; Schreckenbach, G. Theoretical Study of the Oxygen Exchange in Uranyl Hydroxide. An Old Riddle Solved? *J. Am. Chem. Soc.* **2008**, *130*, 13735–13744.

37 Clark, D. L.; Keogh, D. W.; Palmer, P. D.; Scott, B. L.; Tait, C. D. Synthesis and Structure of the First Transuranium Crown Ether Inclusion Complex: $[NpO_2([18]Crown-6)ClO_4$. *Angew. Chem., Int. Ed.* **1998**, *37*, 164–166.

38 Shamov, G. A.; Schreckenbach, G.; Martin, R. L.; Hay, P. J. Crown Ether Inclusion Complexes of the Early Actinide Elements, $AnO_2[18\text{-crown-}6]^{n+}$, An = U, Np, Pu and $n = 1, 2$. A Relativistic Density Functional Study. *Inorg. Chem.* **2008**, *47*, 1465–1475.

39 By an unknown reviewer.

40 We note in passing that two different sets of radii for the solvent cavity (denoted as CPCM and COSMO-PCM, respectively) lead to quite different numerical values for the free energy in solvation. This is not entirely satisfactory, of course. Nonetheless, the general conclusions are supported by either set of data. Moreover, it appears as though the COSMO radii are more accurate for actinide species.

41 Sessler, J. L. *Expanded, Contracted and Isomeric Porphyrins*; Pergamon Press: New York, 1997.

42 Sessler, J. L. Actinide Expanded Porphyrin Complexes. *Coord. Chem. Rev.* **2001**, *216–217*, 411–434.

43 Sessler, J. L.; Melfi, P. J.; Pantos, G. D. Uranium Complexes of Multidentate N-Donor Ligands. *Coord. Chem. Rev.* **2006**, *250*, 816–843.

44 Shamov, G. A.; Schreckenbach, G. A Relativistic DFT Study of Dioxoactinide(VI) and (V) Complexation with Alaskaphyrin and Related Schiff-Base Macrocyclic Ligands. *J. Phys. Chem. A* **2006**, *110*, 9486–9499.

45 Shamov, G. A.; Schreckenbach, G. The Role of the Peripheral Alkyl Substituents: A Theoretical Study of Substituted and Unsubstituted Uranyl Isoamethyrin Complexes. *Inorg. Chem.* **2008**, *47*, 805–811.

46 Liao, M.-S.; Kar, T.; Scheiner, S. Actinyls in Expanded Porphyrin: A Relativistic Density-Functional Study. *J. Phys. Chem. A* **2004**, *108*, 3056–3063.

47 Sessler, J. L.; Seidel, D.; Vivian, A. E.; Lynch, V.; Scott, B. L.; Keogh, D. W. Hexaphyrin(1.0.1.0.0.0): An Expanded Porphyrin Ligand for the Actinide Cations Uranyl (UO_2^{2+}) and Neptunyl (NpO_2^{2+}). *Angew. Chem., Int. Ed.* **2001**, *40*, 591–594.